Molecular Dynamics Simulations of Xe Chemical Shifts and Solubility in *n*-Alkanes†

Huajun Yuan,‡ Sohail Murad,*,‡ Cynthia J. Jameson,‡ and James D. Olson§

Department of Chemical Engineering, University of Illinois at Chicago, 810 S. Clinton, Chicago, Illinois 60607, and The Dow Chemical Company, 770 Building, South Charleston, West Virginia 25303

Received: May 8, 2007; In Final Form: August 13, 2007

Using the molecular dynamics (MD) method, we demonstrate that intermolecular nuclear magnetic resonance chemical shifts can be used to evaluate and develop intermolecular potentials for cross-interactions. We examine the average Xe chemical shifts in *n*-alkanes over a range of temperatures using the optimized potential for liquid simulation all atom force field for the solvent molecules. Comparing the present results with earlier results using nonrealistic rigid model solvent molecules, we obtain chemical shift contributions arising from flexibility of the solvent molecules. Modification of parameters of the exponential-6 potential model for solute−solvent interaction leads to Xe chemical shifts that are in better agreement with experimental values and also leads to improved estimates of Xe solubility. Because the average chemical shift converges in a fraction of the steps necessary to obtain converged solubility, testing of solute−solvent potentials against average chemical shift values, prior to time-intensive calculations of solubility, leads to more efficient development of potentials for mixtures. In the present work the MD simulations reproduce the signs and relative magnitudes of the Xe chemical shifts in *n*-alkanes, as well as the signs and relative magnitudes of their temperature coefficients. A rational comparison of Xe chemical shifts in different solvents can be made when the solvents are in the same thermodynamic state. In an atomistic MD simulation the additive chemical shift contributions arising from the CH_3 and CH_2 groups are obtained separately. We determine these constitutive contributions to the Xe chemical shift for each temperature in each solvent. We find that the per-CH_3 contributions are greater than the per-CH_2 contributions for each case. We also investigate the transferability of these contributions.

Introduction

Increased emphasis is being placed on accurate physical property data and models because of nontraditional applications of physical properties such as biotechnology, polymer solutions, reaction media and solvent selection, environmental applications, product design, and formulation. Industrial projects are driving the need for increasingly complex and faster measurements with smaller samples under difficult conditions. Modeling plays an important role in chemical process simulations, process safety scenarios, product design and formulation, and the need to develop products (lubricants, fuels, etc.) that meet safety standards. The increasing capability and complexity of software for process simulation applications motivates the development and validation of better physical property models. The need for better models, for pure component as well as mixture properties, for industrial purposes was recently described.[1] In particular, it is important to properly account for the effect of underlying fundamental interactions at the molecular level on the macroscopic behavior of fluids. Molecular-based studies of fluids can play an important role in meeting the physical property related needs of the chemical industry. For example, safety standards for storage of flammable liquids require precise knowledge of the amount of O_2 dissolved. Therefore, there is a need for data on the solubility of O_2 in these liquid solvents under various conditions of pressure and temperature. Experimental measurements are precluded under conditions (high temperatures and/or high pressures) close to the flash point. Modeling is a safe alternative, provided that the methods and parameters of molecular level modeling can be validated experimentally. We propose to use a surrogate solute for the O_2 molecule, a solute for which experimental validation can accompany the simulations. We have found that the Xe atom is a suitable surrogate for O_2 for solubility studies.[2,3] In the temperature range where experimental data are available for O_2 and Xe, molecular dynamics (MD) simulations provide accurate values of Henry's constants and gas solubility for O_2 and Xe if we use the same cross-interaction parameter for size in modifying the Lorenz−Berthelot mixing rules. Cross parameters for size have been found to be transferable for similar nonpolar components such as rare gas atoms and small nonpolar molecules such as O_2, N_2, and CH_4.[2] There is the additional motivation that the properties of Xe in liquid solvents are also of intrinsic interest.

Hyperpolarized xenon introduced into blood or tissues provides in vivo chemical-shift selective imaging for medical investigations. Tissue-dissolved hyperpolarized Xe nuclear magnetic resonance (NMR) signals from the thorax and brain have already been observed in rats.[4] These applications depend on the solubility, diffusion, and general interactions of Xe with biologically important molecules.[5] Xenon is highly soluble in lipids and fats and is an anesthetic at subatmospheric pressures.

Because of their relatively simple atomic structure, Xe and the other inert gases have been extensively used to study the solid and liquid states. At the molecular level, xenon atoms in the ground state are spherical with high electric dipole polarizability that enhances dispersion forces, which justify its

† Part of the "Keith E. Gubbins Festschrift".

* To whom correspondence should be addressed. E-mail: murad@uic.edu; phone: (312)-996-5593.

‡ University of Illinois at Chicago.

§ The Dow Chemical Company.

10.1021/jp0735233 CCC: $37.00
Published on Web 10/02/2007

frequent use as a prototype solute in the study of solute−solvent interactions.[6] A series of closely related nonpolar liquids whose molecular structures and properties are well-known can serve as prototype systems to aid in the understanding of gas−liquid solubility. The interactions between Xe and *n*-alkanes, in particular, has been extensively studied.

Experimental measurements by NMR spectroscopy of Xe chemical shifts in a series of liquid hydrocarbons, *n*-alkanes in particular, were reported by Lim and King.[7−9] These authors proposed additive empirical group contributions, suggesting that the Xe chemical shift increases linearly with the increasing fraction of CH_2 groups when Xe chemical shifts in different solvents are compared. This is counter to the theoretical understanding of Xe chemical shift, which would suggest that, based on the number of Xe neighbors, a CH_3 group would provide a greater chemical shift response than a CH_2 group. On the other hand, Bonifacio and Filipe suggested that Lim and King did not take into account that the solvents in which the Xe was dissolved were not in the same thermodynamic states at the same temperature; instead, they compared the measured Xe chemical shifts in solutions at the same reduced temperature and at the same mass density.[10] They found that, for solvents at the same reduced temperature or same mass density, the Xe chemical shifts actually decreased with increasing fraction of CH_2.

In the first MD calculations of Xe chemical shifts in liquids, Jameson, Sears, and Murad[11] used the quantum mechanically calculated nuclear magnetic property for Xe inside cages of water molecules, in cages of various sizes that are surrounded by the first coordination shell of waters, all of which are represented with all electrons. Furthermore, the all-electron calculations are carried out in an array of partial charges that self-consistently provide the correct Madelung potential in the cage in the ice crystal. The latter calculations had quantitatively reproduced the experimental line shapes for Xe in ∼12 types of ice cages found in four different ice structures.[12,13] The quantum mechanical results had been fitted to a suitable functional form, so that for an arbitrary ice configuration the value could be found by summing up Xe−O and Xe−H chemical-shift contributions, which were functions of Xe−O and Xe−H distance.

In liquid solvents, the Xe atom is surrounded by solvent cages that are created and re-formed dynamically. Molecular dynamics provides these configurations of solvent molecules around solute molecules such as Xe. At each time step in MD, the coordinates of all atoms are known; thus, it is easy to calculate any function that depends on the Xe−(solvent atom) distances. Thus, the Xe chemical shift in liquid water was easily found using the simple point charge (SPC) model as the potential function of liquid water.

In the case of Xe dissolved in liquid water, the Xe chemical shift response obtained from quantum mechanical calculations in various hydrogen-bonded cages in ice systems were employed. When no specific hydrogen-bonding or complexation reactions occur in the liquid solvent, the Xe chemical shift response may be more approximately derived from quantum calculations for a system of one Xe atom interacting with one solvent molecule. When this is the case, a similar MD calculation can be done for Xe in any solvent, provided the following: (a) a quantum calculation has been previously done for Xe approaching a single solvent molecule from an adequate set of directions, and this has been fitted to functions of Xe-atom distance [for example, for the solvent CH_3OCH_3, we would need functions of Xe−H, Xe−C, and Xe−O distances]; (b) a potential function is available for the Xe−solvent interactions [in the example, the potential energy could be a pairwise additive function of Xe−H, Xe−C, and Xe−O distances]; and (c) a potential model is available for the solvent−solvent interactions. This potential can be of any form, provided that only the relative distributions of the intramolecular conformations and the intermolecular orientations and distances are reasonably representative of the real liquid. For Xe in alkanes, it was assumed by Sears, Murad, and Jameson that the Xe chemical shift response in $Xe-C_nH_{2n}$ could be replaced with a sum of Xe−C and Xe−H functions of distance, with the C and H being electronically indistinguishable from the C and H in CH_4 insofar as the Xe chemical shift response was concerned.

It is extremely important that the Xe−C and Xe−H potential functions used be compatible with the electronic structure that provides the Xe−C and Xe−H chemical shift response functions. A Lennard−Jones function is not ideal for this purpose because the r^{-12} repulsive part rises too sharply for the proper sampling at those distances, corresponding to the largest chemical shift responses. Therefore, in the past and present work, we use exp-6 functions to describe the Xe−C and Xe−H interactions.

What was inaccurate in the first MD simulations was the use of rigid solvent molecules.[11] All atoms were explicitly taken into account, and degrees of freedom associated with internal rotation were not permitted, however. The conformation of each solvent molecule was first obtained by using a suitable intramolecular force field to minimize the energy. Then, every solvent molecule in the simulation box was fixed at the minimum energy conformation. In the present work, we present a much better description of the dynamic interaction of Xe with the liquid solvent by using molecules that are flexible (able to undergo conformational changes as a standard part of the MD simulations). As a first step in the present simulations of Xe in liquid alkanes, we answer the following question: how large a difference does solvent flexibility make? We can directly compare with the previous work because we are using exactly the same chemical shift functions and the same potential functions for Xe−C and Xe−H.

The Xe chemical shift has been found to be a particularly sensitive probe of the size and shape of pores in solid materials where the atomic level structure of the pores are well-characterized by diffraction methods, such as in clathrate hydrates and zeolite crystals. This is a consequence of the steep dependence of the Xe chemical shift response of the Xe atom to its distance from a neighbor atom; thus, this translates to a strong sensitivity to the configuration of the neighbor atoms around the Xe atom. The difference between Xe in liquids and Xe in porous crystals is that the void spaces in liquids are variable within the time scale of the measurement of the Xe chemical shift. The average Xe chemical shift in liquids is thus an average over the various void sizes and the solvent molecule configurations in the first solvent layer around the Xe atom. The steep dependence of the Xe chemical shift response to the distance from neighbor atoms means that the average is extremely sensitive to the distribution of void sizes and shapes, with the smaller voids being weighted more heavily. Therefore, the Xe chemical shift is a very good probe mainly of the free volume in a liquid but also of the subtle details of the liquid structure.

Because the chemical shift is a sensitive function of configuration of atoms constituting the system, the observed chemical shift is an average over the configurations of the system, weighted according to their relative probabilities. For a solute

TABLE 1: Coefficients for Site−Site Isotropic Chemical Shift Functions Used in This Work, as Defined in Eq 2[11]

n^a	6	8	10	12	14
Xe−C(H_n) c_n(Å^{-n})	−1.482 11 × 10^5	1.045 × 10^7	−1.901 32 × 10^8	1.384 33 × 10^9	−3.455 61 × 10^9
Xe−H h_n(Å^{-n})	8.583 34 × 10^3	6.557 33 × 10^5	1.421 31 × 10^7	−6.347 47 × 10^7	4.200 88 × 10^7

[a] Coefficients for eq. 2.

in a liquid solvent, the average chemical shifts depend on the free volume associated with the liquid structure of the solvent and the solute−solvent intermolecular interactions.[14] Herein lays the connection between the average chemical shifts and the intermolecular interactions. Because the solubility depends on the same factors, there is some expectation that a solute−solvent potential that gives improved chemical shift values will also lead to improved solubility values.

The objective of this paper is to develop a description of Xe in liquid alkanes that can provide accurate values for the solubility. We have already established that the Xe chemical shift reaches a converged average value in a fraction of the MD steps that are required to reach a converged value of the solubility.[14] Therefore, we will use the Xe chemical shift to validate our models for the liquid structure and for the Xe−liquid interactions. In the present work, we find that a small modification in the Xe−liquid potential model improves the agreement of the Xe chemical shift with experiment and at the same time provides improved results for the solubility.

In this paper, we also systematically investigate the variation of Xe chemical shifts in *n*-alkanes, in which the Xe chemical shifts have been measured experimentally as a function of temperature. We carry out Xe chemical shift averaging at various temperatures for each solvent. We seek to discover the underlying physical basis of the magnitudes and signs of the temperature coefficient of the Xe NMR chemical shift in solutions. Furthermore, to clarify the importance of comparing solvents at the same liquid state, rather than at the same temperature and pressure, we investigate the variation of the Xe chemical shifts with the number of carbons in the solvent molecule at corresponding thermodynamic states of the liquids (i.e., at the same reduced temperature). Finally, we examine the basis for a constitutive approach to the chemical shift by investigating the separate CH_3 and CH_2 contributions.

All the solvents considered in the present work are normal (straight chain) hydrocarbons. In a succeeding paper we will investigate the effects of solvent shape on the Xe chemical shift and the solubility.

Methods

Chemical Shift Functions. The observed chemical shift (δ) in solution arises from the difference in shielding (σ) between the free Xe atom (the reference substance) and the isotropic shielding of Xe dissolved in solution (eq 1);

$$\delta = \frac{[\sigma_{(\text{free Xe atom})} - \sigma_{(\text{Xe ininfinitely dilute solution})}]}{[1 - \sigma_{(\text{free Xe atom})}]} \qquad (1)$$

where $\sigma_{(\text{free Xe atom})}$ is small as compared to 1. We can estimate the Xe chemical shift for Xe dissolved in liquid alkanes by assuming that the shielding response of Xe to each C atom of the alkane is the same as the shielding response of Xe to the C atom of a CH_4 molecule and that the shielding response of Xe to each H atom of the alkane is the same as the shielding response of Xe to each H atom of a CH_4 molecule. Furthermore, it is assumed that the overall shielding response of Xe is the additive responses to all atoms within a chosen cutoff distance.

From previous work, we have determined the additive site−site (Xe−C and Xe−H) shielding functions by doing quantum mechanical calculations for a large number of configurations of the $XeCH_4$ supermolecular system.[15] These site−site shielding response functions obtained from Xe@CH_4 are not entirely transferable to Xe@C_nH_{2n+2}; the electronic structure of the C and H atoms within C_nH_{2n+2} is different from that in CH_4, thus make a somewhat different Xe shielding response per C and per H. In a direct comparison of the quantum mechanical calculations for Xe@CH_4 and Xe@H_3CCH_3 for Xe approaching along a direction perpendicular to the H_3C face, the difference between these two calculations is found to be less than 5% at distances that contribute significantly to the average intermolecular chemical shift.[16] Thus, for the MD calculations of Xe chemical shifts for Xe dissolved in liquid alkanes, we will use the Xe−C, Xe−H shielding functions derived from the Xe@CH_4 quantum mechanical calculations. The chemical shift functions used are the site−site additive functions expressed in terms of inverse powers of r_{XeH} and r_{XeC}, referenced to the free Xe atom quantum calculation, of course, in accordance with eq 1. That is, the Xe chemical shift function is expressed as shown in eq 2,

$$\delta = \sum_{H(j)} \sum_{n=6}^{14} h_n r_{\text{Xe}-\text{H}(j)}^{-n} + \sum_{C(k)} \sum_{n=6}^{14} c_n r_{\text{Xe}-\text{C}(k)}^{-n} \qquad (2)$$

where the coefficients are listed in Table 1. The r dependence in each site−site function is adopted from that for intermolecular shielding of two inert gas atoms for which the leading terms do have a physical basis.[17] The pairwise chemical shift function in eq 2 had been constrained to approach the free Xe atom limit (zero) to match the limiting behavior calculated in the supermolecule.[15] Thus, the Xe chemical shift functions have typically gone to zero at much shorter distances than the cutoff distance used in the MD simulation box. For the purposes of this paper, the Xe−C and Xe−H chemical shift functions are considered known and unchanged from the previous work.[11]The averaging implied in eq 1 occurs when the δ value from eq 2 is systematically collected at uniformly spaced MD snapshots.

Potential Functions. For the MD simulations in the *n*-alkanes in this work, an optimized potential for liquid simulation all atom (OPLS-AA) model was chosen to represent the chain molecules of interest. Using the fully flexible potentials in which all the atoms in the molecules are explicitly represented for solvent−solvent potentials has two advantages over other models. The advantage over the united atom model is that we can explicitly include the Xe−H interactions during the simulation and get a more realistic result for the chemical shift and the solubility as well. For example, previous simulation work on the solubility of oxygen in *n*-perfluorohexane [18,19] had demonstrated that the united atom model did not perform as well as the OPLS-AA model. In particular, it was found that the numerical agreement was poorer, and the temperature dependence of the solubility was not reproduced correctly. The advantage of the fully flexible model over the rigid molecule model is that a more realistic distribution of conformations are represented in the simulations.[20] We expect to find out if this has a significant effect on the resulting average chemical shifts.

TABLE 2: OPLS-AA Potential Parameters for Alkanes[21,22]

atom type	q (e$^-$)	σ (Å)	ϵ (kcal/mol)
H	0.060	2.5	0.030
C, RCH_3	−0.180	3.5	0.066
C, R_2CH_2	−0.120	3.5	0.066

bond length

type	r_0 (Å)
C−C	1.529
C−H	1.090

angle bending: $u = k_\theta(\theta-\theta_0)^2$

type	θ_0 (deg)	k_θ(kcal/mol/rad^2)
H−C−H	107.8	33.00
H−C−C	110.7	37.50
C−C−C	112.7	58.35

torsion: $u = k_1(1+\cos\varphi)/2 + k_2(1-\cos 2\varphi)/2 + k_3(1+\cos 3\varphi)/2$

type	k_1 (kcal/mol)	k_2 (kcal/mol)	k_3 (kcal/mol)
H−C−C−H	0.0	0.0	0.3
H−C−C−C	0.0	0.0	0.3
C−C−C−C	1.3	−0.05	0.2

In the model used, the nonbonded potential models adopted for the solvent−solvent interactions are described by the pairwise Lennard−Jones terms plus Coulombic interactions between molecules a and b (eq 3),

$$u_{ij} = \sum_i^a \sum_j^b \left\{ 4\epsilon_{ij}\left[\left(\frac{r_{ij}}{\sigma_{ij}}\right)^{-12} - \left(\frac{r_{ij}}{\sigma_{ij}}\right)^{-6}\right] + q_i q_j / r_{ij} \right\} f_{ij} \quad (3)$$

where ϵ and σ are the Lennard−Jones energy and size parameters, i and j are the active sites, q is the partial charge for the active sites, and r_{ij} is the distance between the active sites i and j. For intramolecular nonbonded interactions, the same expression is used. The factor $f_{ij} = 1.0$, except for intramolecular 1,4 interactions where $f_{ij} = 0.5$, which means that within the same molecule, sites separated by three bonds interact through nonbonded Lennard−Jones and electrostatic terms, similar to the intermolecular ones, but scaled by a factor of 0.5. The parameters were taken from the OPLS-AA force field developed by the Jorgensen group [21] and modified by Chang,[22] as listed in Table 2.

The combining rules for interactions between different species are prescribed by the geometric mean rules for both size and energy parameters (eq 4).

$$\sigma_{ij} = \sqrt{\sigma_{ii}\sigma_{jj}} \qquad \epsilon_{ij} = \sqrt{\epsilon_{ii}\epsilon_{jj}} \quad (4)$$

For the Xe−Xe interaction energy, we use the same parameters as in earlier simulations.[11] The Xe−Xe chemical shift contributions are not included in the chemical shift calculations. Thus, the Xe−Xe interaction is not important except in the behavior of the gas compartment, that is, for the calculation of Henry's constant.

For the Xe−alkane potential, we use the exp-6 model as in previous work (eq 5),[11]

$$u_{\mathrm{Xe}-i} = \sum_i \epsilon_{\mathrm{Xe}-i}\left\{\left(\frac{6}{\alpha_{\mathrm{Xe}-i}-6}\right)\exp[\alpha_{\mathrm{Xe}-i}(1-\bar{r})] - \left(\frac{\alpha_{\mathrm{Xe}-i}}{\alpha_{\mathrm{Xe}-i}-6}\right)\bar{r}^{-6}\right\} \quad (5)$$

TABLE 3: Site−Site Potential Parameters for Xe−Alkane Interactions, as Defined in Eq 5

		$\epsilon/k_B(K)$	α	r_{min} (Å)
previous work[a]	Xe−C_{alkyl}	141.2	16.1	3.99
	Xe−H_{alkyl}	53.3	15.9	3.66
modified, this work	Xe−C_{alkyl}	141.2	16.1	3.75
	Xe−H_{alkyl}	53.3	15.9	3.44

[a] Reference 11.

TABLE 4: Number of Interactions for *n*-Alkanes

number of interactions	Lennard−Jones sites	harmonic bonds	harmonic valence angles	dihedral angles
n-butane (C_4H_{10})	14	13	24	27
n-pentane (C_5H_{12})	17	16	30	36
n-hexane (C_6H_{14})	20	19	36	45
n-octane (C_8H_{18})	26	25	48	63

where $\bar{r} = r_{\mathrm{Xe}-i}/r_{\mathrm{min,Xe}-i}$. The parameters ϵ, α, and r_{min} for Xe−C_{alkyl} and Xe−H_{alkyl} are given in Table 3.

Henry's Constant. During the simulation, we obtained the solubility of Xe in *n*-alkanes. We calculate the Henry's constant via eq 6[23] to include gas phase nonideality as well as the high solvent pressure.

$$H_{12}(T,P_2^{\mathrm{sat}}) = \lim_{x_1\to 0}\left\{\frac{P_1\phi_1}{x_1\exp\{(P_2-P_2^{\mathrm{sat}})\bar{V}_1^{\infty}/RT\}}\right\} \quad (6)$$

Here, T is the temperature, R is the gas constant, x_1 refers to the mole fraction of Xe in the solution, and P_2^{sat} is the equilibrium vapor pressure of the liquid. The pressure (P_1) of the Xe gas phase is estimated from the density (ρ) of the gas phase and the second virial coefficient B using eq 7.

$$P = (1+B\rho)\rho RT \quad (7)$$

The vapor-phase fugacity coefficients (ϕ) can similarly be obtained using eq 8.

$$\ln\phi = 2\rho\mathrm{B} - \ln(P/\rho RT) \quad (8)$$

The pressure in the solvent compartment is calculated from the force on the membranes separating the two compartments, which represents the pressure difference between the two compartments. For Xe we used values of B from ref 24 and values of $\bar{V}_1^{\infty}$ (partial molal volume of the gas dissolved at infinite dilution) from refs 6, 25, and 26.

Molecular Dynamics. The methodology has been described in previous publications,[27,28] so we will only summarize it here. The simulation box consists of a solvent/solution compartment separated from the gas compartment by a semipermeable membrane. A schematic diagram of the simulations is shown in Figure 1. In this method, the membrane typically consists of several layers of atoms arranged in a face-centered cubic (FCC) configuration. In present study, the membrane simply consisted of a single layer of atoms because we were not interested in the dynamic processes occurring during the simulation. The membrane atoms are fixed at their equilibrium positions in an FCC structure. The system is made longer in the x direction (perpendicular to the membranes, $L_x = 4L_y = 4L_z$) to minimize the overall effect of the membranes. The membrane only allows the gas molecules (Xe) to freely permeate it to enter the solution compartment, but prevents the liquid molecules (*n*-alkanes) from moving to the gas compartment. This has been accomplished by adjusting the pore size of the membrane and the intermo-

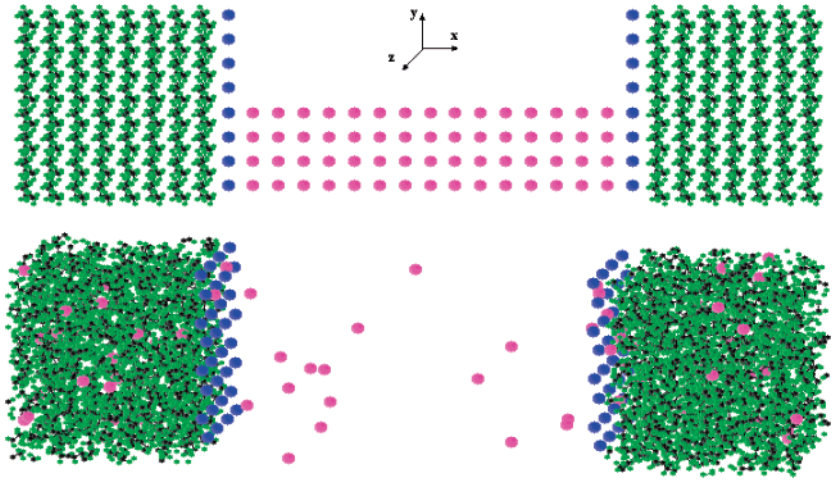

Figure 1. Simulation system for investigating chemical shift and solubility of gas dissolved in liquids at the beginning of the simulation and after equilibration.

lecular interaction between the solvent or gas molecules and the membrane.[27,28]

The density of the solvent compartment can be fixed to correspond to the state condition of interest (experimental density of the liquid alkanes being studied). This fixes the volume of the solvent compartment once the number of molecules to be included in the solvent compartment is specified. Typically, the solution compartment consisted of 480 molecules, and the two membranes consisted of 64 molecules. As adjusted, the density of the liquid in the solution compartment corresponds to the experimental density. In some simulations, some gas molecules were also included in the solvent compartment to facilitate the approach to equilibrium. For convenience, the volume of the gas compartment has been set equal to the solvent compartment (although this is not necessary). The initial number of Xe molecules in the gas compartment is determined by the desired initial pressure of Xe. In general, in our studies we included up to 70 Xe atoms. Because the total number of *n*-alkane molecules in the solution compartment remain fixed during the simulation (the membrane is impermeable to *n*-alkanes) and are at least an order of magnitude larger than the number of Xe atoms in this compartment, the liquid density in the solution compartment remains essentially constant.

The molecules included in the simulation were given a Gaussian velocity distribution[29] corresponding to the system temperature being investigated. The time evolution of this initial system was then followed using a velocity Verlet algorithm[29] using the LAMMPS code.[30] To ensure that our implementation of this code was correct, we did a few simulations using our own MD code for flexible molecules[31] and found that the results from the two programs were in agreement. The initial parameter set for intra- and intermolecular terms were taken from the OPLS-AA force field, for *n*-butane, *n*-pentane, *n*-hexane, and *n*-octane. The Xe−C and Xe−H potential parameters used in our previous work were used in this work. These were then adjusted to improve agreement with experimental values of chemical shift. The original and modified potential parameters are given in Table 3. The number of Lennard−Jones sites and different internal interactions are listed in Table 4.

The temperature was held constant using a Nose/Hoover thermostat.[29] The system was allowed to equilibrate for $1-2 \times 10^5$ time steps. After this, production runs were carried out for $2-4 \times 10^6$ time steps, of size 1×10^{-16} s. Once the simulations were completed, the properties of the system, such as Xe chemical shift, gas pressure, and liquid and gas concentrations,

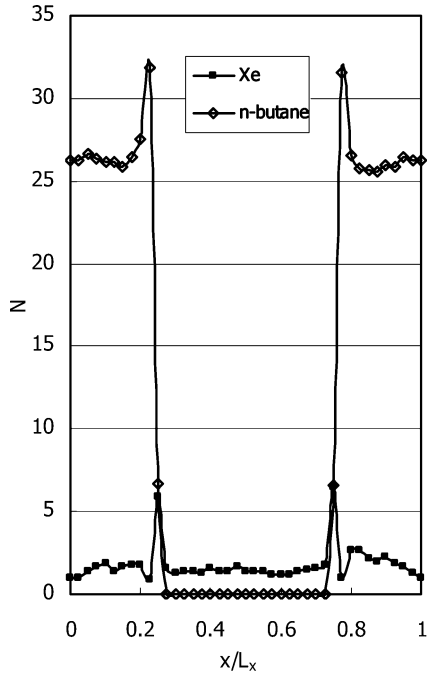

Figure 2. The density profile of solvent and Xe at the end of a typical MD simulation with 3×10^6 steps.

were calculated from the average properties during the latter portions of the production run. A typical density profile from a simulation is shown in Figure 2. The density profile can then be used to estimate both the pressures of the gas and solution compartments and the solubility of the Xe in *n*-alkanes. Using eq 6, Henry's constant can then be calculated.

Results and Discussions

Typical running averages of the Xe chemical shift in one MD run are shown in Figure 3. As the plot shows, the chemical shift converged after about 150,000 time steps, whereas the solubility usually converged after 3 million steps.

Flexible Versus Rigid Alkane Models. Previous MD simulations carried out for Xe in liquids used all-atom rigid models. In the present work, we carried out simulations using the original Xe−alkane potential functions used in previous work and the flexible alkane potentials described above (OPLS-AA with the parameters given in Table 2). In Figure 4, comparison of the MD results at 298 K with experimental values

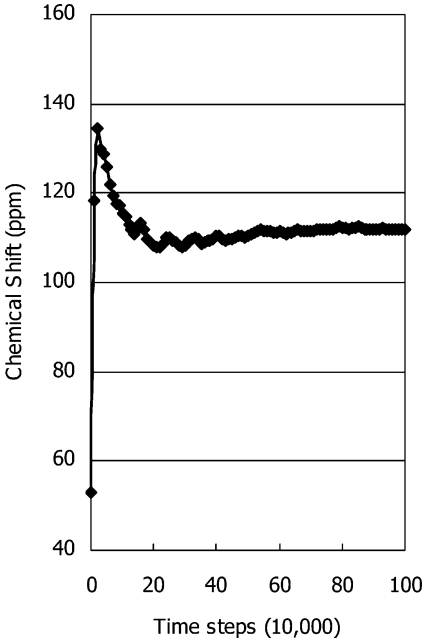

Figure 3. A typical running average of the Xe chemical shift during simulations.

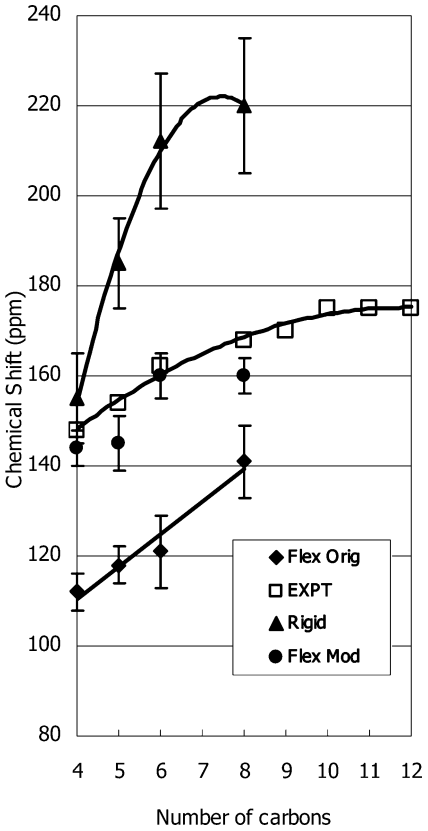

Figure 4. Comparison between average Xe chemical shifts at 298 K, calculated using the original Xe−alkane potential for the rigid model (from ref 11) and the flexible model. Also shown are the results using the modified potential with the flexible model. The experimental values are from ref 7.

clearly indicates that the chemical shifts relative to the reference (free Xe atom at 0 ppm) have the correct sign and correct order of magnitude but are off by 10−30%. As seen in Table 5, the non-realistic all-atom rigid model gives systematically larger chemical shifts than the flexible model, with a more pronounced error for longer chains and also the wrong systematic behavior

TABLE 5: Comparison of Average Xe Chemical Shifts (ppm) at 298 K Calculated Using the Original Xe−Alkane Potential and Using the Flexible Model Compared with the Rigid Model

	chain length	rigid model[a]	flexible model, this work
n-butane	4	170 ± 10	112 ± 4
n-pentane	5	185 ± 10	118 ± 4
n-hexane	6	212 ± 15	121 ± 8
n-octane	8	220 ± 15	141 ± 8

[a] Reference 11.

with chain length at 298 K. From this point on, we abandon the rigid alkane model and use only the flexible alkane model.

The effect of flexibility on the Xe chemical shift is an important finding. There are many confined environments in which Xe has been used as a probe of the internal surface.[32] In some cases, the Xe atoms interact with wall atoms that have fairly stiff, nearly rigid configurations, for example, in crystalline polymers below the glass transition temperature. In other cases, such as in mesoporous channels functionalized with long functional groups, the Xe can become entangled in the flexible chains that are chemically bound to the channel walls.[33] Understanding of the magnitude of the Xe chemical shifts in these environments is possible if various aspects of the environment can be separately considered. All polymers undergo a phase transformation from a soft and rubbery state to a hard and brittle or glassy state as the temperature is lowered below a characteristic glass temperature T_g. It is believed that the transition arises from a stopping or freezing of rotational motions of polymer chain segments. We have shown in the present work that for a given number density, type of functional group, and temperature, flexibility of the neighboring molecular groups can lead to smaller Xe intermolecular chemical shifts as compared to rigid or stiff neighbors. Upon crossing the glass transition temperature, the sharp change in the slope of the decrease in Xe chemical shifts with increasing temperature in polymers [34,35] can therefore be partly attributed to the continuous decrease in the polymer density (and the concomitant increase in free volume) with increasing temperature and partly to the decrease with the onset of increased flexibility of the side chains. The latter is a physical insight we have acquired from the direct comparison of the average Xe chemical shifts from MD simulations at constant density in flexible versus rigid *n*-alkanes in this work.

The Modified Xe−Alkane Potential. The original exp-6 Xe−alkane potential gives Xe chemical shifts that are too small and are found to also give solubilities that are too large. Therefore, we seek to improve the Xe−alkane potential function. The nuclear magnetic shielding for Xe approaching a molecule changes dramatically at shorter distances. Therefore, an intermolecular potential that permits shorter distances to contribute more toward the averaging leads to increasing the intermolecular chemical shift, which improves agreement with experiment. A small modification, as shown in Table 3, has been implemented to do this. The solubility, on the other hand, has no such clear dependence on the intermolecular potential, so the guidance offered by the chemical shift is very useful. Because the Xe chemical shift average converges rapidly, we used it to monitor the effects of changing the potential parameters and calculated the solubility afterward. The agreement of the calculated solubility was indeed found to improve when this change was made. The solubility may improve further when the well depth is changed, but we did not attempt this change because the average chemical shift is known to be less sensitive to the well depth.

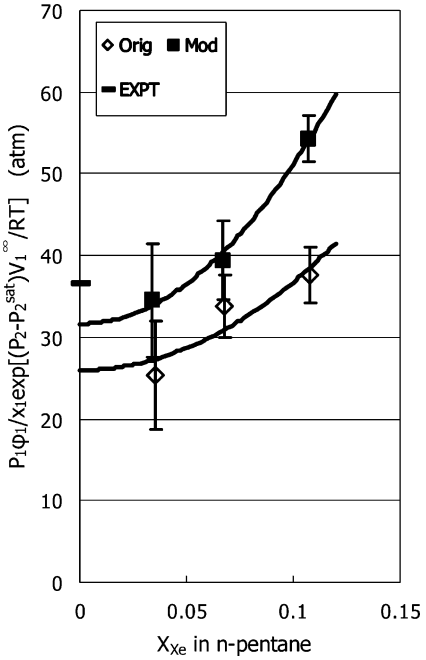

Figure 5. Calculation of Henry's constant using original and modified potential models for Xe in *n*-pentane. The curves extrapolate to the limiting value at zero mole fraction. The experimental value is from ref 36.

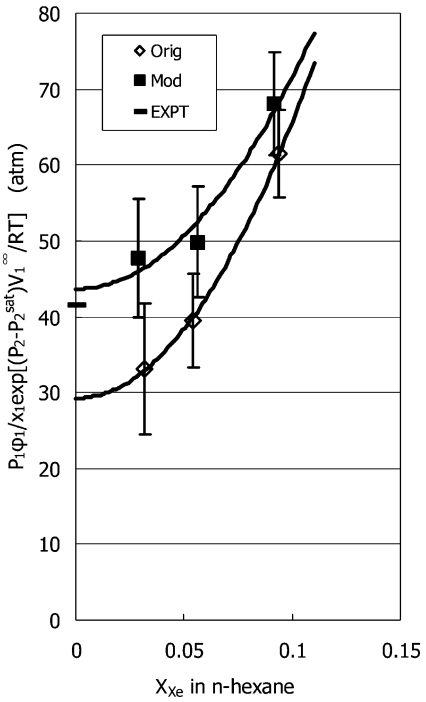

Figure 6. Calculation of Henry's constant using original and modified potential models for Xe in *n*-hexane. The curves extrapolate to the limiting value at zero mole fraction. The experimental value is from ref 36.

Solubility and Henry's Constant. The results for the calculations of the solubilities of Xe in the various *n*-alkanes are shown in Figures 5−7, where the results using the original potential and the modified potential are compared with experimental values. Various mole fractions of Xe in solution are obtained at the end of simulations starting with various initial Xe gas pressures. Henry's constant is obtained by extrapolation of the results to zero mole fraction. We see that there is systematic improvement in the calculated values of the Henry's constant when the modified exp-6 potential is used. Even more convincing is the temperature dependence of the Henry's constant obtained using the modified exp-6 potential. These are compared against the experimental temperature dependence for Xe in *n*-hexane in Figure 8.

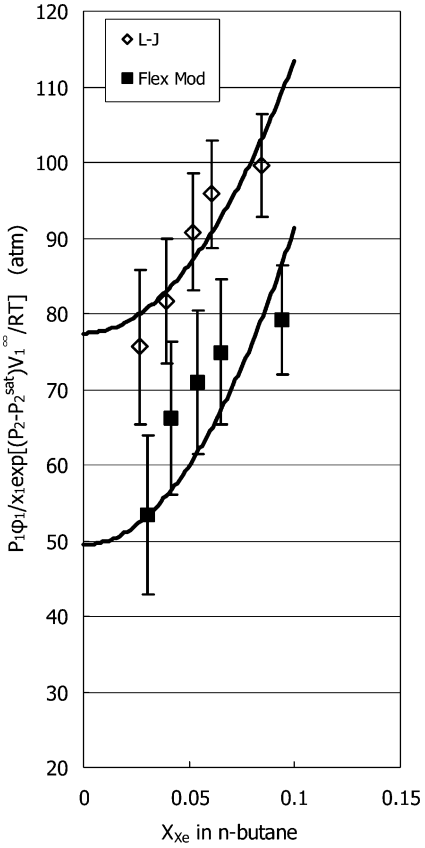

Figure 7. Calculation of Henry's constant using different potential models for Xe in *n*-butane. The curves extrapolate to the limiting value at zero mole fraction.

Results for *n*-pentane are shown in Figure 5. The experimental value of Henry's constant is approximately 37 ± 7 (estimated from the solubility at 1 atm). The original potential model (not fitted to the chemical shift) gives an extrapolated result of 26 ± 7, whereas for the modified potential (fitted to the chemical shift), the Henry's constant is 32 ± 7. Thus, the modified potential leads to a significant improvement (beyond the experimental and simulation uncertainty). A similar improvement is seen for *n*-hexane, for which results are shown in Figure 6. The reported experimental value is 39 ± 6, whereas the extrapolated values from the original and modified potentials are 29 ± 10 and 44 ± 8, respectively, once again showing a significant improvement. These improvements, although impressive, are not unexpected. The chemical shift is strongly dependent on the cross-molecular interaction between the solute and solvents, as is the Henry's constant. Most potentials currently available are fitted to vapor−liquid data that are not as sensitive to the cross-interactions. No experimental data is currently available for butane, but it has been estimated to be 37 ± 7 by extrapolating results for other hydrocarbons.[36] The simulated values for the Lennard−Jones and the modified exp-6 potentials, shown in Figure 7, are 77 ± 7 and 49 ± 8, respectively. In this particular case, the Lennard−Jones potential does quite poorly, but the modified exp-6 potential continues to accurately represent the behavior of a dilute solution of Xe in *n*-butane.

A final crucial and important test of a potential model is its ability to correctly estimate the temperature dependence of

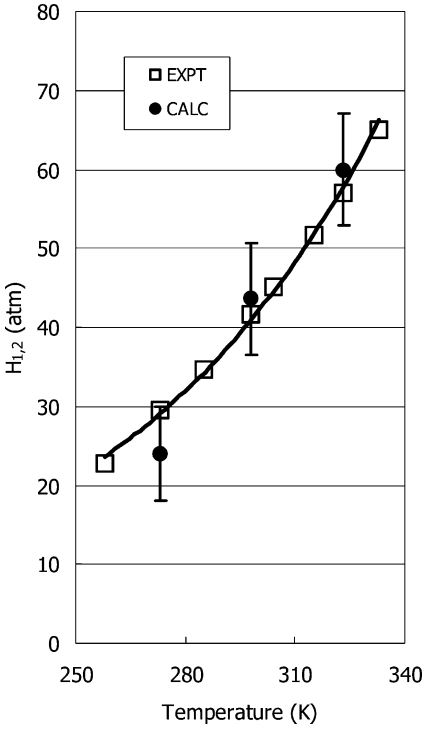

Figure 8. Temperature dependence of Henry's constant for *n*-hexane compared with experimental data from ref 36.

Henry's constant. This behavior is notoriously difficult to theoretically estimate[1,3] because the behavior varies from substance to substance and depends on whether the enthalpy of solution of a solute in a solvent is positive or negative as well as its magnitude. This property depends upon the ability of a theory to correctly predict a small difference between two larger quantities, which explains why many theories have trouble correctly predicting enthalpies of solutions.[37] For example, the Henry's constant of oxygen in benzene decreases as the temperature increases, whereas it increases in hexane in the temperature range 283−323 K.[38] The results for the temperature dependence of Henry's constant are shown for *n*-hexane in Figure 8. The results show a remarkable agreement between the experimental temperature dependence and the simulated values. This reinforces our belief that potential models fitted to the chemical shift are remarkably accurate for gas solubility and Henry's constants. A summary of all our results for Henry's constant for both models is given in Table 6, and the trend with the number of carbons is shown in Figure 9.

From this point on, we use only the modified exp-6 Xe-alkane potential function shown in Table 3. The final MD values for the average Xe chemical shifts in various liquids at 298 K are given in Table 7. The agreement with experimental values is good.

The Temperature Dependence of the Xe Chemical Shift. The Xe chemical shift has been measured in a number of *n*-alkanes from pentane to hexadecane at atmospheric pressure as a function of temperature in the 170−330 K range.[10] The measured chemical shifts change linearly with temperature for all studied alkanes, exhibiting uniformly negative temperature coefficients ranging from −0.37 ppm K^{-1} for *n*-pentane to −0.31 for *n*-hexane, *n*-octane, and *n*-nonane and −0.27 for *n*-tetradecane and *n*-hexadecane. The results of the MD simulations in *n*-pentane and *n*-hexane in the present work do exhibit linear temperature dependences of the Xe chemical shift, with negative temperature coefficients that are comparable to the experimental values from Bonifacio et al.,[10] as seen in Figures 10 and 11. Tables 8 and 9 compare the MD values at selected temperatures for *n*-hexane and *n*-pentane with experimental values at these temperatures. Below, we consider the mechanism for the experimental and MD findings that the temperature dependences are linear, are substantial, and exhibit a negative temperature coefficient.

In a constant density experiment, such as the measurement of the Xe chemical shift in a sealed sample of a mixture of Xe and other gases, the temperature dependence arises entirely from the Boltzmann factor that provides the probability of a particular configuration of Xe with the other molecules. The average Xe chemical shift measured under such conditions contains information about the intermolecular interaction potential function. The average Xe chemical shift for infinitely dilute Xe in an infinitely dilute gas of density ρ_B consisting of B molecules is given by eq 9,

$$\langle\delta(\mathrm{Xe{-}B})\rangle = \delta_1(T, \mathrm{Xe{-}B}) \times \rho_B \tag{9}$$

where the second virial coefficient $\delta_1(T, \mathrm{Xe{-}B})$ is given by eq 10.

$$\delta_1(T, \mathrm{Xe{-}B}) = \int \{2\pi[\sigma_{\mathrm{Xe-B}}(r=\infty, \theta) - \sigma_{\mathrm{Xe-B}}(r, \theta)] \exp^{-V(r,\theta,T)/k\mathrm{BT}} r^2 \, \mathrm{d}r \sin\theta \, \mathrm{d}\theta\} \times (1 \times 10^{-24}\ \mathrm{cm^3/\AA^3})(6.022 \times 10^{23}\ \mathrm{molecules/22\,414\ cm^3}) \tag{10}$$

Because $\exp^{-V(r,\theta,T)/k\mathrm{BT}}$ is only the first term in the pair distribution function, this expression for $\delta_1(T, \mathrm{Xe{-}B})$ is only valid for a very dilute gas. For Xe infinitely dilute in higher densities of B, we need the higher-order terms shown in eq 11.

$$\langle\delta(\mathrm{Xe{-}B})\rangle = \delta_1(T, \mathrm{Xe{-}B})\rho_B + \delta_2(T, \mathrm{Xe{-}B})\rho_B{}^2 + \delta_3(T, \mathrm{Xe{-}B})\rho_B{}^3 + \ldots \tag{11}$$

Such measurements have been reported for Xe since the early 1970s.[39] The nonlinear terms become significant for number densities of more than 200 amagats and provide a correction opposite in sign to the linear term.[40] (One amagat is the number density of an ideal gas at standard temperature and pressure.) The temperature dependence of the second virial coefficient of the intermolecular chemical shift $[\delta_1(T, \mathrm{Xe{-}B})]$ has also been measured for several B molecules.[41−43] For Xe infinitely dilute in B gas at temperature *T*, we obtain eq 12,

$$\langle\delta(\mathrm{Xe{-}B})\rangle = [N_B/V] \int \{2\pi[\sigma_{\mathrm{Xe-B}}(r=\infty, \theta) - \sigma_{\mathrm{Xe-B}}(r, \theta)] g(r, \theta, T) \, r^2 \, \mathrm{d}r \sin\theta \, \mathrm{d}\theta\} \tag{12}$$

where $g(r, T)$ is properly normalized according to the following equation.

$$V_{\mathrm{box}} = 4\pi \int \{g(r, T) \, r^2 \, \mathrm{d}r\} = \text{volume of simulation box in } \mathrm{\AA^3}$$

The number density is given by eq 13,

$$[N_B/V] = n_B(1 \times 10^{-24}\ \mathrm{cm^3/\AA^3})(6.022 \times 10^{23}\ \mathrm{molecules/22\,414\ cm^3}) \tag{13}$$

where n_B equals the number of amagats. For constant volume experiments in the gas phase, this is a constant. In contrast, solution experiments are typically carried out at constant

TABLE 6: Henry's Constant (atm) for Xe in *n*-Alkanes at 298 K Calculated Using the Original and the Modified Exp-6 Potential, Compared with Experiment

	n-butane	*n*-pentane	*n*-hexane	*n*-octane	nonane	decane	undecane
No. of carbons	4	5	6	8	9	10	11
calc orig exp-6	LJ 77 ± 7	26 ± 7	29 ± 10				
calc. mod. exp-6	49 ± 8	32 ± 7	44 ± 8				
experiment[a]	37[b]	37	39	40	40	40	41

[a] Estimated from solubility at 1 atm from ref 36. [b] Estimated by extrapolation of experimental values for the *n*-alkanes

TABLE 7: Xe Chemical Shifts (ppm) in *n*-Alkanes at 298 K Calculated Using the Modified Exp-6 Potential, Compared with Experiment

	n-butane	*n*-pentane	*n*-hexane	*n*-octane	nonane	decane	un-decane
# carbons	4	5	6	8	9	10	11
calc.	144 ± 4	148 ± 8	159 ± 7	164 ± 7			
experiment[a]	145.4	154.1	160.3	169.8	171.7	175.6	176.0

[a] Reference 7.

TABLE 8: Temperature Dependence of the Xe Chemical Shifts (ppm) in *n*-Pentane Calculated Using the Modified Exp-6 Potential and Compared with Experiment[a]

	200 K	235 K	298 K
calc	189 ± 12	174 ± 8	148 ± 8
experiment[a]	190	178	154

[a] Additional experimental values are shown in Figure 10. [b] Reference 10.

TABLE 9: Temperature Dependence of the Xe Chemical Shifts (ppm) in *n*-Hexane Calculated Using the Modified Exp-6 Potential and Compared with Experiment[a]

	200 K	254 K	273 K	298 K	323 K
calc.	205 ± 16	175 ± 5	168 ± 5	159 ± 7	153 ± 8
experiment[b]	192	175	171	162	153

[a] Additional experimental values are shown in Figure 11. [b] Reference 10.

pressure, so the number density of solvent in a sample changes with temperature.

If we write the Xe intermolecular shift in solvent B as eq 14,

$$\langle \delta\,(\mathrm{Xe{-}B})\rangle = n_{\mathrm{B}}\delta_{1,\mathrm{effective}}(\mathrm{Xe{-}B}) \qquad (14)$$

then we get eq 15,

$$\delta_{1,\mathrm{effective}}(\mathrm{Xe{-}B}) = 4\pi \int \{[\sigma_{\mathrm{Xe-B}}(r=\infty,\theta) - \sigma\,(r_{\mathrm{Xe-B}})]g\,(r_{\mathrm{Xe-B}}, T) r_{\mathrm{Xe-B}}{}^2\,\mathrm{d}r_{\mathrm{Xe-B}}\}(1\times 10^{-24}\ \mathrm{cm}^3/\mathrm{\AA}^3)(6.022\times 10^{23}\ \mathrm{molecules}/22\,414\ \mathrm{cm}^3) \qquad (13)$$

in ppm amagat^{-1} is the effective second virial coefficient for the Xe chemical shift in liquid B. For Xe infinitely dilute in a liquid, the measurement of the temperature dependence under conditions of constant liquid density has to be carried out in a sample system capable of withstanding high pressures. Although much work has been carried out by Jonas and co-workers in many liquids,[44] none of them involve solutions of Xe. All reported temperature-dependent Xe chemical shift measurements in liquid solvents are under constant pressure conditions.[45,7−9] In an MD simulation such as in this work, the temperature dependence of the average Xe chemical shift can be obtained under constant pressure conditions for direct comparison with experimental measurements. Under such experimental conditions, the dominant temperature dependence of the Xe chemical shift arises from the number density rather than from the intrinsic temperature dependence of the effective second virial coefficient $\delta_{1,\mathrm{effective}}$ (the density coefficient). For a given solvent, a first-order estimate of the temperature coefficient of the Xe chemical shift can thus be easily obtained from the temperature coefficient of the liquid density. For the liquid *n*-alkanes, the liquid density at atmospheric pressure is found to decrease linearly with increasing temperature.[46] This largely accounts for the observed negative temperature coefficient of the Xe chemical shift, provided that the temperature dependence of $\delta_{1,\mathrm{effective}}$ for Xe chemical shift is not significantly large. The MD results easily provide the latter. We find that the effective second virial coefficient for Xe chemical shift changes with temperature in a systematic way for all the *n*-alkanes in our study, as shown in Figure 12. We see that factoring out the solvent density at room temperature does permit a more sensible comparison of different solvents because this permits a physical understanding of the experimental magnitudes and sign of the temperature coefficients of Xe chemical shifts in solution, and it permits the separation of the large part of the temperature dependence, which can be attributed entirely to the change of number density, with temperature from the smaller temperature dependence seen in Figure 12, which arise from the temperature dependence of the intermolecular interactions, that give rise to the chemical shift response. While the chemical shifts in *n*-pentane and *n*-hexane change by 25% in the given temperature range, the $\delta_{1,\mathrm{effective}}$ for Xe chemical shift in these solvents only change by 7%. The mechanism for the large, nearly linear temperature dependence of the Xe chemical shift observed in organic solvents under typical NMR measurement conditions is thus largely the expansion of the liquid with increasing temperature, in addition to the smaller effect because of the change in the intermolecular interactions with temperature.

TABLE 10: Xe Chemical Shifts (ppm) in *n*-Alkanes at $T^* = 0.5$,[a] Calculated Using the Modified Exp-6 Potential and Compared with Experiment[b]

	n-butane	*n*-pentane	*n*-hexane	*n*-octane
T_c	425	470	507	569
T	213	235	254	285
calc.	182 ± 3	174 ± 8	175 ± 5	171 ± 8
experiment[c]		178	175	174

[a] $T^* = T/T_c$, where T_c is the critical temperature. [b] Additional experimental values for higher alkanes are shown in Figure 13. [c] Reference 10.

The effects on Xe chemical shifts of the size, branching, and chemical functionality in various solvents can appear to be anti-intuitive when the experimental values are compared at the same (room) temperature. We have established with MD simulations that the appropriate comparison is for the various solvents in the same thermodynamic state. A way to compare Xe chemical

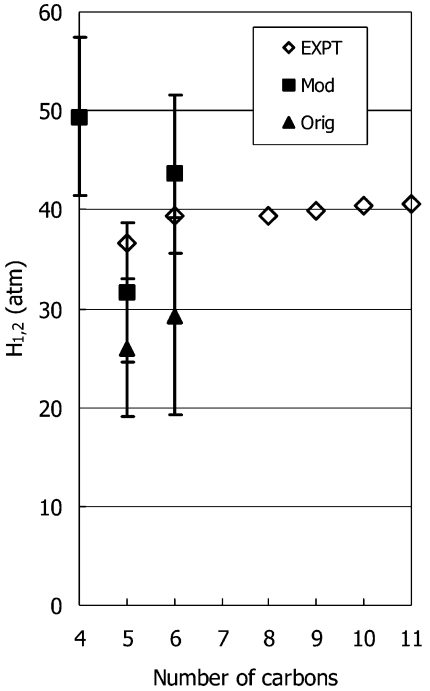

Figure 9. Comparison of Henry's constants calculated using original and modified potential models for Xe in *n*-alkanes against experimental values from ref 36.

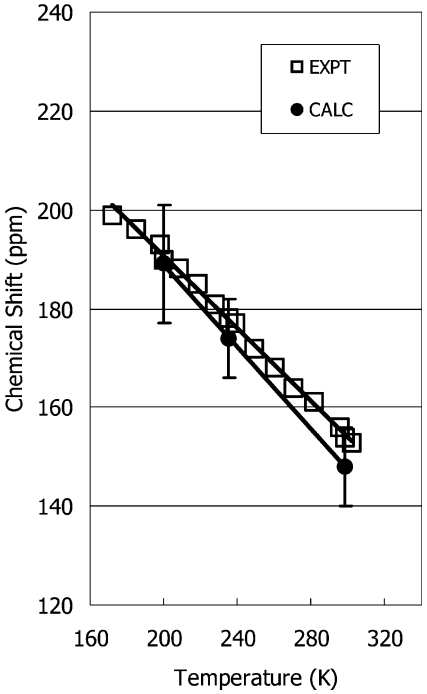

Figure 10. Temperature dependence of the Xe chemical shift in *n*-pentane. Experimental data are from ref 10.

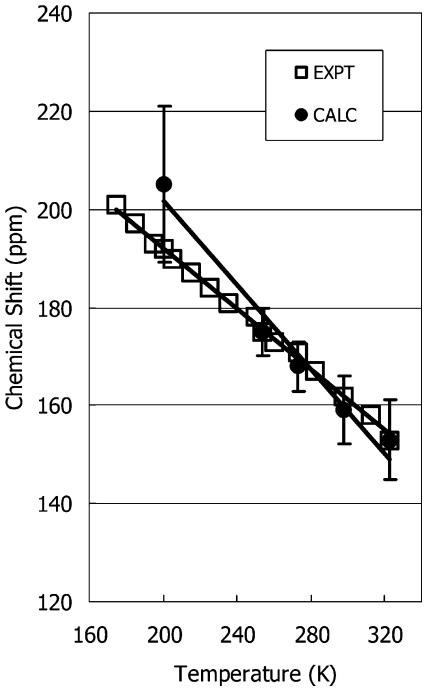

Figure 11. Temperature dependence of the Xe chemical shift in *n*-hexane. Experimental data are from ref 10.

shifts in different solvents at comparable thermodynamic states is to examine the chemical shifts in solutions at the same reduced temperature (T^* is defined here as T/T_c), as suggested by Bonifacio et al.[10] These authors have shown their experimental data for Xe chemical shift in *n*-alkanes with 5, 6, 8, 9, 14, and 16 carbons at $T^* = 0.5$. They found that, unlike the Xe chemical shift at 298 K that is markedly increasing with increasing chain length, at the same T^* the Xe chemical shift is nearly independent of chain length, only slightly decreasing with increasing chain length. Our MD simulations at $T^* = 0.5$ for Xe in *n*-alkanes with 4, 5, 6, and 8 carbons reveal that the Xe chemical shift is nearly independent of chain length. Table 10 provides a comparison of the average values obtained from the MD simulations with those from experiments. The slight decrease with increasing chain length is almost within the error bars of the simulation, as shown in Figure 13. We also have the values of $\delta_{1,\text{effective}}$ at $T^* = 0.5$, and these are 0.69, 0.83, 0.96, and 1.32 ppm amagat^{-1} for Xe in *n*-butane, *n*-pentane, *n*-hexane, and *n*-octane, respectively. These magnitudes increase with the number of carbons in the solvent molecule, as expected, and as we shall see below, these magnitudes can be reconstituted from nearly constant CH_3 and CH_2 contributions.

The Dependence of the Xe Chemical Shift on the Number of C Atoms and CH_2 Content of the Solvent. The effective second virial coefficient in eq 13 contains the information regarding separate contributions of CH_3 and CH_2 chemical groups (for example) of the solvent molecule to the observed Xe chemical shift, when we use a chemical shift function that is additive site−site, as in this work. The number density at a given temperature also depends on the mass of the molecule for a given molecular type and on the number of CH_2 groups per molecule, when comparing *n*-alkanes, for example. Thus, if an empirical constitutive scheme is to be devised for the empirical prediction of Xe chemical shifts in different liquids, measured Xe chemical shifts in liquids can be compared with each other only at the same reduced temperature so as to properly scale according to corresponding liquid states. Likewise, different liquids can be compared with each other only at the same mass density if an empirical constitutive scheme is to be extracted from the data at the same temperature. Thus, the comparisons used by Lim et al. in attempting to devise a constitutive scheme for group contributions to the Xe chemical shift in liquids are inherently flawed, leading to the false conclusion that a CH_2 group provides a larger Xe chemical shfit contribution than a CH_3 group, because they were comparing various liquids at different thermodynamic states.[7−9] The suggested comparisons by Bonifacio and Filipe of various liquid solvents at the same reduced temperature or at the same mass density at a fixed temperature are much more sensible.[10] These lead to the conclusion that the CH_3 group provides a larger Xe

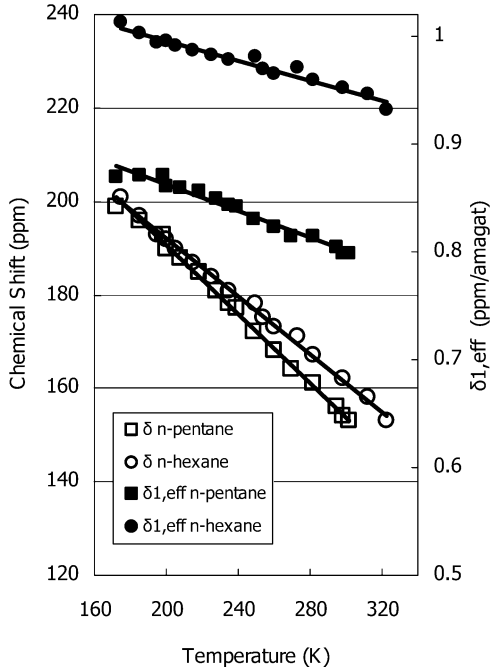

Figure 12. Temperature dependence of the effective second virial coefficients of the Xe chemical shifts $\delta_{1,\text{effective}}$, ppm amagat^{-1} in *n*-pentane and *n*-hexane, from experimental chemical shifts in ref 10, which are also shown.

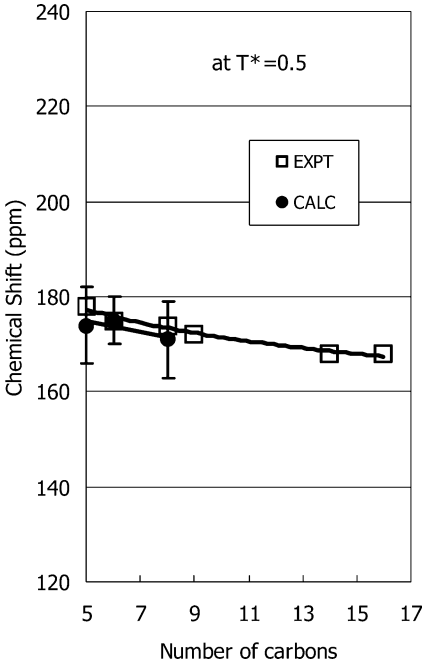

Figure 13. Xe chemical shifts in *n*-alkanes at reduced temperature $T^* = 0.5$. Experimental data are from ref 10.

chemical shift contribution than a CH_2 group. Another suggestion was made by Luhmer and Bartik;[47] they simply divide the experimental Xe−solvent shift at 293 K by the empirical liquid density and assume that the density coefficient for the Xe−solvent intermolecular shifts can be expressed as constitutive group contributions. This leads to the conclusion that the CH_3 group provides a larger Xe chemical shift contribution than a CH_2 group at 293 K. In particular, for the liquid *n*-alkanes, they found that the empirical contributions are 3.95 and 3.29 ppm M^{-1} for CH_3 and CH_2, respectively, which is a ratio of 1.20 for 293 K. Using this method, they found that the CH_2 contributions to the density coefficient appear to be the same for linear alkanes, linear alkyl alcohols, acids, and dialkyl ketones. However, for cycloalkanes a much smaller value of 2.52 ppm M^{-1} was arrived at for 293 K. They suggested that this must be because of the different arrangements of CH_2 groups in cycloalkane solvent molecules around the Xe atom.

Empirically defined constitutive contributions depend on the set of molecules that are included in the fitting. Unlike the empirical definitions used by Lim et al.,[7] or Luhmer et al.,[47] the constitutive group contributions derived from an atomistic MD simulation of chemical shifts do not result from a fitting of experiments. Using flexible molecules, the MD simulations properly take into account the distributions of solvent molecule configurations around the Xe atom during the MD run. The Xe−H and Xe−C chemical shift contributions separately arising from the CH_3 and CH_2 groups are well-defined by separate sums within an MD run. This means that we can determine these constitutive contributions to the Xe chemical shift (or its effective second virial coefficient $\delta_{1,\text{effective}}$(Xe−B)) for each liquid solvent and for each temperature via MD calculations. Comparisons among the solvent molecules of MD results for the CH_3 and CH_2 contributions to the Xe chemical shift (or to $\delta_{1,\text{effective}}$(Xe−B)) will reveal whether they are indeed transferable from one solvent to another, without making the a priori assumption of transferability that was assumed by Lim et al.[7] and Luhmer and Bartik.[47] These comparisons can provide physical insight that may permit estimation of such values for other functional groups. The temperature dependence of the constitutive contributions will also provide physical insight; this involves the nature of the liquid dynamics and the temperature dependence of the conformational distributions. Comparisons between solvents can be made at the same reduced temperature, as suggested by Bonifacio and Filipe.[10]

One of the possible physical insights to be drawn from the above comparisons is the effect of the accessibility of the functional group in the solvent molecule on its contribution to $\delta_{1,\text{effective}}$(Xe−B). For example, end groups have a distinct advantage in contributing to the Xe chemical shift because of the site effect. This means that the CH_3 group contribution to the effective second virial coefficient of the Xe chemical shift in the solvent should be larger than CH_2, not only because there are more atoms contributing to the sum of Xe responses, but also because of the site effect. The site effect was illustrated very clearly in the gas-phase second virial coefficients measured for ^{19}F intermolecular chemical shifts in CF_2═CFX for each of X = H, F, Cl, Br, and I.[48] Which of the ^{19}F sites (trans, cis, or gem to the X substituent) is the more exposed one depends on the mass of X, if we assume that the molecule is freely rotating about its center of mass. It was found that the experimental $\delta_1(^{19}\text{F})$ was systematically larger for the more exposed ^{19}F in each of the CF_2═CFX gases. In a similar manner, the CH_3 groups at the ends of the *n*-alkane molecule are more exposed to Xe than the CH_2 groups in the linear alkyl chain. Thus, the nuclear site effect should lead to CH_3 contributions that are larger than the CH_2 contributions to the $\delta_{1,\text{effective}}$(Xe−B) in the solvent molecule B. Likewise, the CH_2 groups in a linear alkyl chain are more exposed to Xe than the CH_2 groups in cycloalkanes. We expect that the constraints associated with the cyclic geometry will keep the CH_2 from getting as close to the Xe atom, as does the CH_2 in a linear chain. All these physically reasonable predictions can be validated by examining the Xe−other atom pair distributions that are routinely collected in MD simulations. There is, of course, the actual electronic difference between the C and H response contributions from CH_3 groups as opposed to CH_2 groups, and the electronic

TABLE 11: Constitutive Contributions to Xe Chemical Shift (ppm) for Xe in *n*-Alkanes

	$T = 298$ K				$T^* = 0.5$			
solvent	*n*-butane	*n*-pentane	*n*-hexane	*n*-octane	*n*-butane	*n*-pentane	*n*-hexane	*n*-octane
No. of carbons	4	5	6	8	4	5	6	8
CH_3	42.2	39.4	33.1	30.1	53.1	46.1	39.7	30.5
CH_2	28.9	26	21.7	18.1	37.7	30.2	24.7	19.7
ratio	1.46	1.51	1.52	1.66	1.41	1.53	1.61	1.55

TABLE 12: Constitutive Contributions to $\delta_{1,\text{effective}}$(Xe−B) (ppm Amagat^{-1}) for Xe in *n*-Alkanes

	$T = 298$ K				$T^* = 0.5$			
solvent B	*n*-butane	*n*-pentane	*n*-hexane	*n*-octane	*n*-butane	*n*-pentane	*n*-hexane	*n*-octane
No. of carbons	4	5	6	8	4	5	6	8
CH_3	0.192	0.198	0.190	0.222	0.202	0.209	0.215	0.225
CH_2	0.131	0.131	0.125	0.134	0.144	0.137	0.134	0.146

TABLE 13: Prediction of Xe Chemical Shifts (in Ppm) in *n*-Alkanes ($n = 9-16$) at 298 K from CH_3 and CH_2 Contributions to $\delta_{1,\text{effective}}$(Xe−B) (ppm Amagat^{-1}) Derived from MD of Xe in *n*-Alkanes ($n = 4-8$)

solvent B	*n*-nonane	*n*-undecane	*n*-dodecane	*n*-tetradecane	*n*-hexadecane
No. of carbons	9	11	12	14	16
prediction using $\delta_{1,\text{effective}}(CH_3) = 0.20$ and $\delta_{1,\text{effective}}(CH_2) = 0.13$ based on MD at 298 K	164	167	167	169	170
prediction using $\delta_{1,\text{effective}}(CH_3) = 0.21$ and $\delta_{1,\text{effective}}(CH_2) = 0.14$ based on MD at $T^* = 0.5$	175	179	179	182	183
experiment[a]	171.7	176.0	176.6	180.7	182.8

[a] Reference 7.

difference between the C and H response contributions from CH_2 groups in cycloalkanes and *n*-alkanes. However, we do not reflect this at all in our simulations because we assume all H atoms to be electronically equivalent and all C atoms to be electronically equivalent for the alkanes in the present study.

The constitutive contributions from CH_2 and CH_3 groups are obtained directly from the MD simulations as described above and are shown in Table 11. The first important result shown in Table 11 is that, by separately averaging the contributions to the Xe chemical shift, we have established that the per CH_3 group contribution is larger than the per CH_2 group contribution for each of the Xe−alkane solutions at 298 K. This shows that the constitutive analysis by Lim and King,[7−9] which led to the conclusion that CH_2 contributions are greater than CH_3 contributions, is faulty. The second important result is that the per CH_3 group contributions at 298 K (likewise for the per CH_2 group contributions) are different for each alkane. That is, the contributions to the Xe chemical shift are not quite transferable from one alkane to another. Third, the ratio of the CH_3 to the CH_2 contributions in each molecule range from 1.4 to 1.66. This is in good agreement with the physical arguments based on site effect and numbers of atoms in the group but is in marked contrast to the reported CH_3 to CH_2 contributions ratio of 0.5 from Lim and King.[7]

Last, from our MD simulations we can directly obtain the group contributions to $\delta_{1,\text{effective}}$, as shown in Table 12. We find that at 298 K the contributions to $\delta_{1,\text{effective}}$ are nearly constant and are therefore approximately transferable, supporting the assumption of transferability made in the constitutive analysis carried out by Luhmer and Bartik.[47] However, our CH_3 and CH_2 contributions are in a ratio closer to 1.5 or larger, as compared to Luhmer and Bartik's empirically deduced ratio of 1.20. The final important result in Table 12 is that the CH_3 (and CH_2) contributions to $\delta_{1,\text{effective}}$ at $T^* = 0.5$ are nearly constant and therefore can be considered transferable from one alkane to another. To test the transferability, we used the average of our MD values of CH_3 and CH_2 contributions to $\delta_{1,\text{effective}}$ to predict the Xe chemical shift of the higher alkanes from their experimental density. The results are shown in Table 13. We find from their densities at 298 K that we can obtain, in each case, a reasonable value for the Xe chemical shift at 298 K in nonane, undecane, dodecane, tetradecane, and hexadecane. The predictions are much better if we use the average CH_3 and CH_2 contributions obtained from the simulations at $T^* = 0.5$. Thus, the CH_3 and CH_2 group contributions in Table 12 are more nearly transferable from one alkane to another when the liquids are compared at the same thermodynamic state (e.g., at $T^* = 0.5$). Thus, we recommend the values 0.21 and 0.14 ppm amagat^{-1} for CH_3 and CH_2 group contributions to $\delta_{1,\text{effective}}$, respectively.

Conclusions

We have investigated the Xe chemical shift in infinitely dilute solutions in *n*-alkanes. The most important finding is the utility of the Xe chemical shift as a test of Xe−alkane potentials. Because the average intermolecular chemical shift of the solute is closely related to the local environment, and because the averaging of the chemical shift converges in a fraction of the number of steps necessary to obtain a converged solubility, testing of solute−solvent potential models against average chemical shift values, prior to time-intensive calculations of solubility, leads to more efficient development of potentials for mixtures. Our results show that potential parameters that lead to improved average chemical shifts provide improved estimates for the solubility and Henry's law constants. Because the average Xe chemical shift converges in a fifth of the simulation time as compared to solubility, it provides an efficient means of testing of potentials prior to solubility simulations.

This study has shown that flexibility of solvent molecules greatly influences the average Xe chemical shift. For a given density, temperature, and chemical composition, solvent flexibility leads to lower Xe chemical shifts as compared to those calculated using rigid groups. This is an important finding that provides insight into applications of Xe in probing pores with pendant groups attached to the walls, such as functionalized mesopore channels and polymers. The temperature dependence of the Xe chemical shift in typical experimental measurements

has been analyzed in terms of the major mechanism (the linear decrease of the density with increasing temperature leads to a linear decrease of the Xe chemical shift with the temperature) and a secondary mechanism (the temperature dependence of the intermolecular interactions lead to a change of the effective second virial coefficient of Xe chemical shift with temperature). From our simulations we can separate out the mechanisms for the temperature dependence by looking at the effective second virial coefficient of the Xe chemical shift.

We have shown that the apparent large change in the magnitude of the Xe chemical shift in alkanes with increasing number of carbon atoms at room temperature is a consequence of incorrectly comparing solutions that are not in the same thermodynamic state. The dependence of the Xe chemical shift with the number of carbons in the *n*-alkane chain is not very pronounced, provided we compare the chemical shift values in liquids at the same thermodynamic state, such as at the same reduced temperature. The relative magnitudes of these CH_2 and CH_3 contributions are in the order $CH_3 > CH_2$ (a ratio of 1.4−1.6), which makes physical sense when one takes into account the three rather than two H atoms providing the chemical shift response and also the greater exposure of Xe to the end groups (CH_3) as opposed to the middle groups (CH_2), in agreement with a previously documented nuclear site effect. Previous analyses of chemical shift data at the same temperature (not at the same thermodynamic state) had erroneously arrived at the opposite order for CH_3 and CH_2 contributions, which did not make physical sense. Further studies with branched alkanes and cycloalkanes should permit us to determine how much of the $CH_3 > CH_2$ difference comes from the site effect and how much comes from the differing number of H atoms. We have found that the nearly constant CH_2 and CH_3 contributions to the density coefficient of the Xe chemical shift from our work can be used to predict reliable Xe chemical shifts in other linear alkanes.

Acknowledgment. This research has been funded by the National Science Foundation [Grant Nos. CHE-9978259 (CJJ), CTS-0314203 (SM)], the Department of Energy [Grant No. DE-FG02-96ER14680 (SM)], and a grant from the American Chemical Society (Petroleum Research Fund).

References and Notes

(1) Gupta, S.; Olson, J. D. *Ind. Eng. Chem. Res.* **2003**, *42*, 6359.
(2) Krishnamurthy, M.; Murad, S.; Olson, J. D. *Mol. Simul.* **2006**, *32*, 11.
(3) Murad, S.; Gupta, S. *Fluid Phase Equil.* **2001**, *187*, 29.
(4) Swanson, S. D.; Rosen, M. S.; Coulter, K. P.; Welsh, R. C.; Chupp, T. E. *Magn. Reson. Med.* **1999**, *42*, 1137.
(5) Cherubini, A.; Bifone, A. *Prog. Nucl. Magn. Reson. Specrosc.* **2003**, *42*, 1.
(6) Bonifacio, R. P.; Costa Gomes, M. F.; Filipe, E. J. M. *Fluid Phase Equil.* **2002**, *193*, 41.
(7) Lim, Y. H.; King, A. D. *J. Phys. Chem.* **1993**, *97*, 12173.
(8) Lim, Y. H.; Nugara, N.; King, A. D. *J. Phys. Chem.* **1993**, *97*, 8816.
(9) Lim, Y. H.; Nugara, N.; King, A. D. *Appl. Magn. Reson.* **1995**, *8*, 521.
(10) Bonifacio, R. P.; Filipe, E. J. M.; Nunes, T. G. XEMAT2000 Proceedings, 28−30 June, 2000, Sestri Levante, Italy.
(11) Jameson, C. J.; Sears, D. N.; Murad, S. *J. Chem. Phys.* **2004**, *121*, 9581.
(12) Stueber, D.; Jameson, C. J. *J. Chem. Phys.* **2004**, *120*, 1560.
(13) Jameson, C. J.; Stueber, D. *J. Chem. Phys.* **2004**, *120*, 10200.
(14) Jameson, C. J.; Murad, S. *Chem. Phys. Lett.* **2003**, *380*, 556.
(15) Sears, D. N.; Jameson, C. J. *J. Chem. Phys.* **2004**, *121*, 2151.
(16) Moudrakovski, I.; Soldatov, D. V.; Ripmeester, J. A.; Sears, D. N.; Jameson, C. J. *Proc. Natl. Acad. Sci., U.S.A.* **2004**, *101*, 17924.
(17) Jameson, C. J.; de Dios, A. C. *J. Chem. Phys.* **1993**, *98*, 2208.
(18) Padua, A. A. H.; Deschamps, J.; Marrucho, I.; Sarraute, S.; Costa Gomes, M. F. 13th European Symposium on Fluorine Chemistry, Bordeaux, France, 15−20 July, 2001
(19) Dias, A. M. A.; Bonifácio, R. P.; Marrucho, I. M.; Pádua, A. A. H.; Costa, Gomes, M. F. *Phys. Chem. Chem. Phys.* **2003**, *5*, 543.
(20) Gupta, S.; McLaughlin, E. *Mol. Phys.* **1990**, *70*, 433.
(21) Jorgensen, W. L.; Maxwell, D. S.; Tirado-Rives, J. *J. Am. Chem. Soc.* **1996**, *118*, 11225.
(22) Chang, J.; Sandler, S. I. *J. Chem. Phys.* **2004**, *121*, 7474.
(23) Prausnitz, J. M.; Lichtenthaler, R. N.; Gomes de Azevedo, E. *Molecular Thermodynamics of Fluid Phase Equilibria*, 3rd ed.; Prentice Hall: New Jersey, 1986.
(24) Dymond, J. H.; Smith, E. B. *The Virial Coefficients of Gases, A Critical Compilation*; Clarendon Press: Oxford, 1969.
(25) Pollack, G. L. *J. Chem. Phys.* **1981**, *75*, 5875.
(26) Filipe, E. J. M.; Martins, L. F. G.; Calado, J. C. G.; McCabe, C.; Jackson, G. J. *Phys. Chem. B* **2000**, *104*, 1322.
(27) Murad, S.; Gupta, S. *Fluid Phase Equilib.* **2001**, *29*, 187.
(28) Murad, S.; Gupta, S. K. *Chem. Phys. Lett.* **2000**, *60*, 319.
(29) Allen, M. P.; Tildesley, D. J. *Computer Simulation of Liquids*; Oxford University Press: Oxford, 1989.
(30) Steve Plimpton and co-workers, Large-scale Atomic/Molecular Massively Parallel Simulator (LAMMPS) MD code; Sandia National Laboratories, Department of Energy.
(31) Jia, W.; Murad, S. *Molec. Phys.* **2006**, *104*, 3033.
(32) Bonardet, J. L.; Fraissard, J.; Gedeon, A.; Springuel-Huet, M. A. *Catal. Rev.-Sci. Eng.* **1999**, *41*, 115.
(33) Huang, S. J.; Huh, S.; Lo, P. S.; Liu, S. H.; Lin, V. S. Y.; Liu, S. B. *Phys. Chem. Chem. Phys.* **2005**, *7*, 3080.
(34) Cheung, T. T. P.; Chu, P. J. *J. Phys. Chem.* **1992**, *96*, 9551.
(35) Walton, J. H. *Polym. Polym. Compos.* **1994**, *2*, 35.
(36) Clever, H. L. *IUPAC Solubility Data Series, Krypton, Xenon and Radon-Gas Solubilities*, Pergamon Press: Oxford, 1976; Vol. 2.
(37) Mysels, K. J. *J. Chem. Ed.* **1955**, *32*, 399.
(38) Battino, R. *IUPAC Solubility Data Series*; Pergamon Press: Oxford, 1981; Vol. 7, p 250.
(39) Jameson, A. K.; Jameson, C. J.; Gutowsky, H. S. *J. Chem. Phys.* **1970**, *53*, 2310.
(40) Jameson, C. J.; Jameson, A. K.; Cohen, S. M. *J. Chem. Phys.* **1973**, *59*, 4540.
(41) Jameson, C. J.; Jameson, A. K.; Cohen, S. M. *J. Chem. Phys.* **1975**, *62*, 4224.
(42) Jameson, C. J.; Jameson, A. K.; Cohen, S. M. *J. Chem. Phys.* **1976**, *65*, 3401.
(43) Jameson, C. *J. Chem. Rev.* **1991**, *91*, 1375.
(44) Jonas, J. *Acc. Chem. Res.* **1984**, *17*, 74.
(45) Stengle, T. R.; Reo, N. V.; Williamson, K. L. *J. Phys. Chem.* **1981**, *85*, 3772.
(46) *Densities of Aliphatic Hydrocarbons: Alkanes*. Landolt-Börnstein − Group IV Physical Chemistry, Numerical Data and Functional Relationships in Science and Technology; Springer−Verlag: Berlin, 1996; Vol. 8B.
(47) Luhmer, M.; Bartik, K. *J. Phys. Chem. A* **1997**, *101*, 5278.
(48) Jameson, C. J.; Jameson, A. K.; Oppusunggu, D. *J. Chem. Phys.* **1984**, *81*, 2313.